Research Article

Sensitivity study of planetary boundary layer scheme in numerical simulation of western disturbances over Northern India

Abhijit Sarkar[1] · Abhijit Sarkar[2] · Susmita Majumdar[3] · Devajyoti Dutta[1]

Abstract
A numerical weather forecasting model (WRF-ARW) is used to simulate the weather during western disturbances over India. The horizontal resolution of the model is 27 km, and the model covers a region extending from 40°E to 105°E and 10°N to 48°N. The Asymmetric Convective Model, version 2 (ACM2) scheme is used to parameterize planetary boundary layer in the simulations. This scheme uses several parameters which are hidden or implicit from the model users. Literature shows that a particular parameter '*p*' used in this scheme to prescribe the vertical profile of eddy exchange coefficient has significant impact on mixing within the planetary boundary layer. Thus, the default value of '*p*' may not be the most appropriate choice for all types of atmospheric conditions. In the present study, attempt has been made to study the effect of '*p*' on the parameters like potential temperature and relative humidity within planetary boundary layer and also to prescribe an appropriate value of '*p*' for the region under study. Our study reveals that the WRF-ARW model embedded with PBL parameterization (ACM2) is capable of more appropriately simulating the potential temperature and relative humidity by using '*p*' value of 1.25 to prescribe the vertical profile of eddy exchange coefficient within the boundary layer especially during the daytime when the system is dominated by convective-scale eddies at least for the chosen domain and period of study.

Keywords Numerical simulation · Planetary boundary layer · Parameterization scheme · Western disturbance

1 Introduction

Planetary boundary layer (PBL) is the lowermost portion of the atmosphere roughly constituting 1–3 km of the lower troposphere region and is characterized by friction and vertical mixing [1, 2]. Hydrometeorological process and dispersion of pollutants occurring within this PBL region are strongly dependent on the turbulent vertical mixing, and thus a good representation of vertical mixing in the planetary boundary layer (PBL) is important for modeling of meteorological and air quality phenomena. In numerical mesoscale modeling, it is vital to account for the subgrid-scale processes occurring within the confine of model grid for improving the model performance when the processes are not explicitly resolved in the model at coarser resolution. Since the scale of turbulent mixing is relatively smaller than the model resolution, the overall impact due to turbulent forcing on grid-scale variables of meteorology and air pollution is expressed through PBL parameterizations in numerical models. During the past few decades, various turbulent vertical mixing schemes for use in the PBL were developed and tested in 1D and 3D simulations in both meteorological and air quality modeling-related studies. These vertical mixing schemes can be local schemes or *K*-schemes [3–6], non-local vertical mixing schemes [7–10] or may be combination of local and non-local schemes [11]. Studies conducted by most of these schemes [12, 13] infer that

✉ Devajyoti Dutta, devankaster@gmail.com | [1]National Centre for Medium Range Weather Forecasting (NCMRWF), A-50, Sector-62, Noida, Uttar Pradesh, India. [2]Department of Environmental Science, Tezpur University, Tezpur, Assam, India. [3]Galgotias University, Greater Noida, Uttar Pradesh, India.

SN Applied Sciences (2019) 1:173 | https://doi.org/10.1007/s42452-019-0177-1

Received: 9 October 2018 / Accepted: 9 January 2019 / Published online: 21 January 2019

modeling is sensitive to the vertical mixing scheme and appropriate apportion of flux between local and non-local component is crucial in representing mixing occurring within the PBL. The turbulence mixing can occur in a wide range of scale starting from subgrid scale to a scale as high as to the depth of the convective boundary layer. Performance of these PBL schemes in numerical weather prediction models varies with respect to the physics options, geography of the study region and time of the year [14–17]. Therefore, careful examination of these schemes for a chosen domain is crucial to not only weather prediction and research, but also for air quality studies and other environmental investigations [18]. Atmospheric boundary layer representation during convective condition of atmosphere has long been a quest area in numerical simulation of meteorological processes and air quality prediction [10]. The subgrid-scale processes, viz. mixing of heat, momentum and moisture, occurring in the atmospheric boundary layer primarily take place through convective and mechanical forcing of the earth surface due to differential heating and cooling during the daytime and nighttime, respectively. Sensitivity experiments with different local (e.g., *K*-theory in Stull [1]) and non-local PBL schemes show that complex phenomenon occurring within the boundary layer is likely to affect the vertical mixing within the PBL and evolution of PBL parameters which ultimately influence the air quality dispersion of the region [19–21]. Performance of near-surface PBL structure variation is more influenced by the surface layer formulation, whereas the upper profile of PBL is more influenced by mixing algorithms of parameterization schemes [22]. Results also indicate that there is a large variation in the mixing layer height estimated by the model using different combinations of surface and PBL schemes [23]. All the above studies show that appropriate representation of vertical mixing occurring within the confine of planetary boundary layer is thus one of the important components which needs our keen attention for meteorological and air quality modeling under different conditions of atmosphere and geography. Moreover, uncertainty associated with the PBL schemes remains one of the key sources of inaccuracy in model simulations [12, 24]. Inadequate parameterizations of physical processes or faulty parameter estimation cannot be justified by merely optimizing the initial and boundary condition [25]. Data assimilation techniques enable us to improve the accuracy of parameterizations in PBL schemes by estimating the most appropriate value of the model parameter. Parameter estimation using variational data assimilation method and ensemble Kalman filter are robust approaches to deal with model error associated with incorrect parameter value in PBL scheme [26–28]. It is also appropriate to say that parameterization of subgrid-scale meteorological process often ends up with range of a model parameter values which need to be optimized for the chosen domain of study. Therefore, parameters optimized for specific purpose within a PBL scheme are not essentially confined to the constant values assigned in the parameterization formulation under different spatial and temporal domains. Hence, it is also important to optimize the parameter values intended for parameter estimation over specific temporal and spatial domains. A numerical weather forecasting model like WRF-ARW offers several options of parameterization schemes for different physical processes. Routinely Planetary Boundary Layer (PBL) schemes are appropriately used to parameterize the vertical turbulent fluxes of heat, momentum and moisture within the planetary boundary layer as well as in free atmosphere. Within these PBL schemes, there are many less known hidden or implicit parameters which govern the mixing within the boundary layer. Each parameterization scheme contains several parameters which can vary over a range of values, and the choice of a value of parameter may depend on the geographical and meteorological conditions. One of such parameter in ACM2 [11, 24] scheme is '*p*' which appears in the model equation to express the eddy exchange coefficient K_z in non-local closure scheme. This parameter is believed to govern the local mixing profile within the unstable portion of the boundary layer. It determines the maximum value of K_z and the height at which K_z will be maximum. Study carried out by Nielsen-Gammon et al. [25] also states that among all the parameters, '*p*' has maximum impact on the vertical mixing in the boundary layer during the daytime. Thus, sensitivity study with a suitable choice of implicit or less known parameters in the boundary layer parameterization schemes is crucial for accurate simulation of extreme weather conditions, especially when the system is dominated by convective-scale eddies. However, it is also appropriate to admit that performance of different meteorological variables in numerical model also depends on combination of different physical processes like cumulus convection, cloud microphysics and definition of model initial state in the simulation of low temperature, strong wind and heavy precipitation [29]. In order to evaluate the dependency, sensitivity experiments need to be carried out to determine the most appropriate value of '*p*' for the region of study. Thus, the objective of the present study is to accurately simulate the meteorological variables such as potential temperature and relative humidity by modifying these parameters in the boundary layer parameterization scheme suitable for the chosen region of study.

Subgrid-scale turbulent fluxes of heat, momentum and moisture within the planetary boundary layer are expressed in terms of mean quantities and their gradients with the help of turbulent closure method in the PBL scheme. A local closure scheme is more appropriate in a stable atmosphere than in an atmospheric condition where the turbulent fluxes are dominated by large eddies. Since an extreme weather event like western disturbance is characterized by large-scale advective and convective types of phenomena, the local closure schemes will produce insufficient mixing. Thus, in contrast, a non-local scheme will be more appropriate to use the profile of eddy diffusivity and incorporates the non-local effect of transport by the large eddies in the model. Besides, the counter-gradient fluxes are also taken into consideration by the non-local approach. It is also considered to be more robust numerically as stability oscillations do not affect it considerably [30].

This paper is organized as follows. Section 2 provides a description of the model, and Sect. 3 provides the configuration of the simulations. In Sect. 4, the results are presented, mainly focusing on the comparison of the simulation results with observations or analyses. Section 5 formulates the conclusions.

Table 1 Overview of the ARW model configuration used for the present study

Number of domains	2
Horizontal grid distances	27 km, 9 km
Integration time step	Adaptive
Number of grid points	*X*-direction—231 points (40°E to 105°E) *Y*-direction—160 points (10°N to 48°N)
Vertical coordinate	Terrain-following hydrostatic-pressure coordinate (38 level) η values at the model levels are: 1, 0.99734, 0.99165, 0.98522, 0.97793, 0.96973, 0.96049, 0.95012, 0.93849, 0.92552, 0.91106, 0.89506, 0.87739, 0.85797, 0.83674, 0.81366, 0.78872, 0.76194, 0.73339, 0.70319, 0.67148, 0.63846, 0.60438, 0.56950, 0.53415, 0.49863, 0.39437, 0.29953, 0.21939, 0.15579, 0.10778, 0.07289, 0.04823, 0.03115, 0.01948, 0.01157, 0.00625, 0
Model top	10 mb
Microphysics	Lin et al. [39] scheme
Cumulus parameterization schemes	Kain–Fritsch scheme
Radiation scheme (long wave)	RRTM scheme
Radiation scheme (short wave)	Dudhia's short-wave radiation
Surface layer physics	Monin–Obukhov scheme
PBL parameterization	ACM2 scheme
Time integration	Runge–Kutta second- and third-order time integration scheme
Spatial differencing scheme	Second- and sixth-order differencing scheme
Map projection	Mercator
Initial and boundary conditions	Three-dimensional real-data (FNL: 1°×1°)

2 Model description

Weather Research and Forecasting (WRF) is a non-hydrostatic, fully compressible numerical weather prediction (NWP) model designed by National Center for Atmospheric Research (NCAR) in collaboration with National Centers for Environmental Prediction (NCEP) and several other institutes. It is a community model and has been developed for both the research and operational applications. The WRF Software Framework (WSF) contains the dynamic solvers, physics packages, programs for initialization, WRF-Var and WRF-Chem. WSF has two dynamic solvers: the Advanced Research WRF (ARW) solver and the Non-hydrostatic Mesoscale Model (NMM) solver. ARW has been developed primarily at NCAR and NMM at NCEP. In the present study, version 3.3 of ARW has been used. A brief description of the model configuration used for the present study is given in Table 1. ARW uses a terrain-following hydrostatic-pressure vertical coordinate, η. A detailed technical description of ARW is available in [31]. WRF model has been very widely used over a range of applicability and operability and has been tested effectively in forecasting extreme rainfall event [32, 33], inter-comparison of winter and non-winter hail storms [34], sensitivity of physical schemes in simulating intense western disturbances [35] and meteorological data source for dispersion modeling [36].

3 Methodology

In the present study, nine cases of western disturbances (WD) that occurred during the winter seasons between 2005 and 2009 are chosen and simulated by using WRF-ARW model keeping the model horizontal resolution at 27 km. Figure 1 shows the model domain. Table 1 states the nine cases that have been investigated in the present study.

The NCEP FNL (Final) Operational Global Analysis data of 1°×1° resolution have been used as model initial and lateral boundary conditions. The static geographical input data of resolution 30″, 2, 5′ and 10′ that include MODIS, GWD, SSiB and VARSSO data have been downloaded from official Web site of WRF. In each case mentioned in Table 2, the model integration starts at 00:00 UTC of the previous day. As an example, in case 1, the weather condition of January 11, 2007 has been investigated. The model run starts with initial condition of 00:00 UTC of January 10,

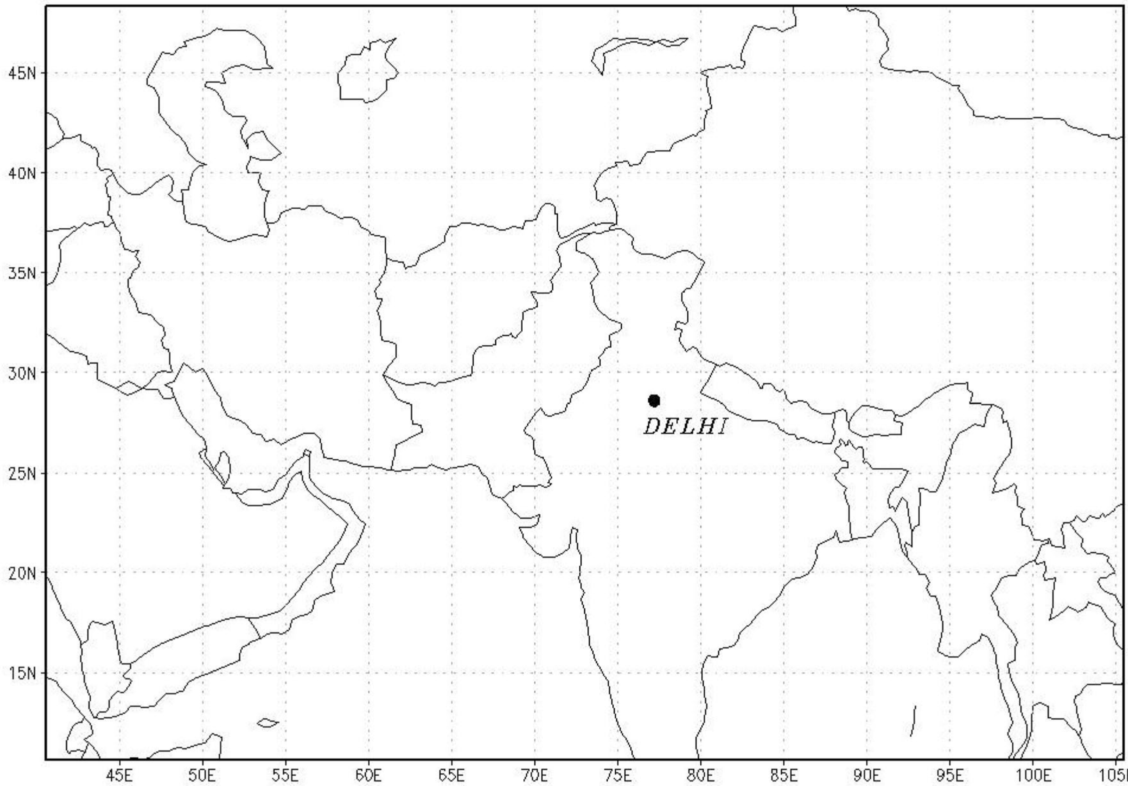

Fig. 1 Model domain of study

Table 2 Dates of the WD cases simulated in the present study

Case	Date of event
1	January 11, 2007
2	December 12, 2007
3	January 15, 2007
4	January 02, 2006
5	February 04, 2005
6	January 01, 2005
7	December 8, 2008
8	December 17, 2008
9	December 9, 2009

2007. Model result obtained after 24 h model run has been used for analysis. Lateral boundary condition gets updated at an interval of 6 h.

A coarse horizontal grid of size 27 km cannot resolve subgrid-level phenomena; thus, parameterization schemes are required to represent the subgrid-scale processes. In the present case, cumulus parameterization is necessary to take care of latent heat release on a realistic timescale in the convective column. The modified version of the Kain–Fritsch scheme [37] has been chosen as the cumulus parameterization scheme in the WRF-ARW model system. It uses a simple cloud model with moist updrafts and downdrafts, which include the effects of detrainment, entrainment and relatively simple microphysics. This modified version of the Kain–Fritsch scheme is different from the original KF scheme [38] in many ways which is briefly described in the technical note of ARW version 3.

Lin et al. [39] scheme has been chosen as cloud microphysics scheme for this study. It has been taken from Purdue cloud model. The Lin et al. scheme includes six classes of hydrometeors. These hydrometeors are water vapor, cloud water, rain, cloud ice, snow and graupel. It uses the bulk water microphysical parameterization technique to represent the precipitation fields which follow exponential size distribution functions. The detailed description of this scheme is available in Chen and Sun [40].

For the present investigation, the asymmetric convective model, version 2 (ACM2) scheme has been used as planetary boundary layer parameterization scheme to simulate various cases of western disturbances in WRF-ARW model. ACM2 can better represent the shape of the vertical profiles of model variables, especially the gradually decreasing gradient near the surface. ACM2 has been chosen for our experiments as comparatively lower bias was reported in the sensitivity experiments than other non-local PBL schemes [12]. This PBL parameterization scheme has been included in WRF-ARW model very recently. ACM2 is a non-local model and it considers the non-local fluxes explicitly through a transilient term [9]. This scheme contains several parameters which can vary over a range of values, and the choice of a value of a parameter may depend on the geographical and meteorological circumstances.

Local time derivative of potential temperature (θ) in the PBL scheme proposed by Deardorff [41], Holtslag and Boville [5] and others can be represented by

$$\frac{\partial\theta}{\partial t} = \frac{\partial\left(\overline{w'\theta'}\right)}{\partial x} = \frac{\partial}{\partial z}\left[-K_{\text{h}}\left(\frac{\partial\theta}{\partial z} - \gamma_{\text{h}}\right)\right] \tag{1}$$

where K_h is the vertical eddy diffusion coefficient of heat, γ_h is the gradient adjustment term and $\overline{w'\theta'}$ is the kinematic heat flux. Similar equation is applicable for humidity also. In asymmetrical convective model, ACM1 [9] mass fluxes are represented by rapid upward convective non-local transport from the lowest model layers directly to all other layers but gradual downward asymmetric layer-by-layer transport. Provision of local upward diffusion from one layer to the next layer is absent in ACM1 which is unrealistic. Pleim [11, 24] has described the formulation of ACM2 which combines the non-local scheme of ACM1 with an eddy diffusion scheme to represent turbulent transport of mass, moisture and heat within a convective boundary layer.

In ACM2 scheme, a weighting factor f_{conv} controls the mixing due to local diffusion and non-local transport. $f_{conv}=0$ corresponds to fully local mixing and $f_{conv}=1$ corresponds to fully non-local mixing. For stable and neutral conditions, the portion of mixing due to non-local transport becomes zero and this scheme handles vertical mixing by pure local eddy diffusion component.

In ACM2, the PBL scaling form of vertical eddy diffusion coefficient K_z within the planetary boundary layer is represented as

$$K_z = k\left(\frac{u_*}{\varphi}\right)z\left(1 - \frac{z}{h}\right)^p \tag{2}$$

where k = the von Karman constant, u_* = friction velocity, φ = similarity profile function, z = height above ground level and h = height of the top of PBL measured from the ground level.

From Eq. 2, it can be seen that there are many parameters that affect the vertical mixing in this scheme. Values of these parameters used in this scheme are kept hidden from WRF-ARW model users. Different roles played by these parameters and their plausible values are tabulated in Nielsen-Gammon et al. [25]. The detailed investigation of Nielsen-Gammon et al. [25] reveals that among the ten parameters, 'p' plays the most important role in governing the vertical mixing in the daytime. This parameter (p) determines the value of the local eddy vertical mixing coefficient within the convective PBL, with larger p leading to smaller vertical mixing.

The parameter 'p' used in Eq. (2) is also a hidden parameter, and by default the value of 'p' used in the model is 2. The prescribed plausible range of 'p' values lies between 1 and 3. It is clear from Eq. (2) that 'p' determines the height at which eddy diffusivity becomes maximum. For $p=1$, eddy diffusivity becomes maximum at the middle of the boundary layer. This height decreases with the increase of 'p' value. Thus, eddy diffusivity is determined by the magnitude of 'p'. A smaller value of 'p' refers to stronger mixing. Figure 2 shows the vertical profiles of normalized K_z for different values of 'p' with PBL height arbitrarily set at 2000 m. This shows that vertical eddy diffusivity K_z varies considerably with the 'p' values and hence the vertical mixing strength in daytime within the PBL is largely dependent on the p value.

Selection of most appropriate value of hidden parameter 'p' through sensitivity experiments is important as 'p' influences the vertical mixing mostly within the PBL. The present study aims at finding out the impact of the variation of p values on boundary layer during WDs and the most appropriate value of 'p' for simulation of western disturbance over the region of study. Two variables that are mostly affected by the variation of vertical mixing are potential temperature (θ) and relative humidity (RH). The resultant effect due to change of 'p' values will be studied on them. Since the vertical profile form of K_z is applicable in the daytime boundary layer, the behavior of potential temperature (θ) and relative humidity (RH) profile within daytime boundary layer will be discussed. Thus, model outputs are taken at 00, 06, 12 and 18 UTC and the θ and RH profiles at 06 UTC are expected to be influenced most by the variation of p values. In the present study, six values of 'p' between 1 and 3 were chosen. These values are 1.25, 1.50, 1.75, 2.0, 2.50 and 2.75.

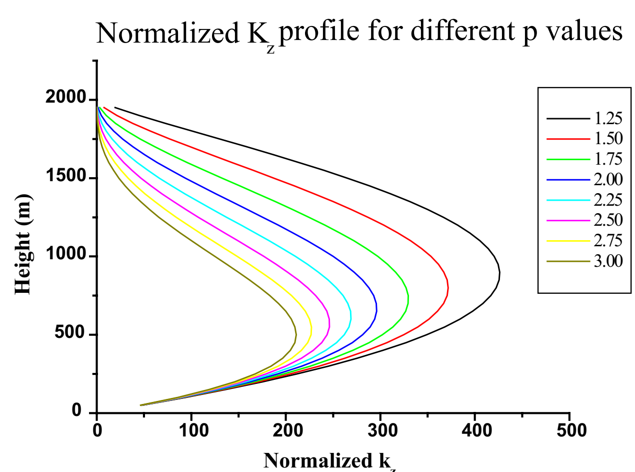

Fig. 2 Normalized profiles of K_z for different values of p

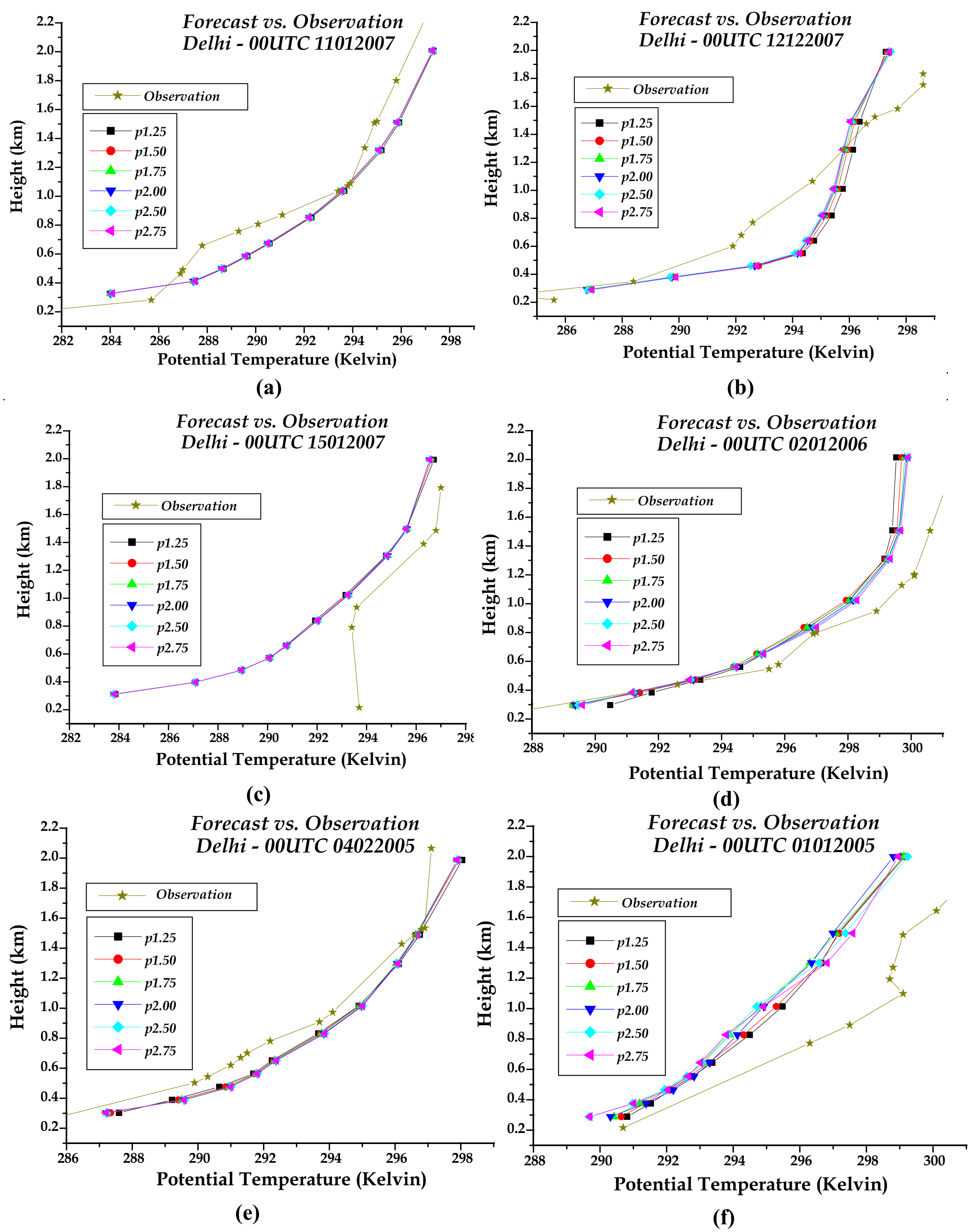

Fig. 3 Potential temperature profile at 00:00 UTC at Delhi for six cases

4 Results and discussion

4.1 Impact of '*p*' values on potential temperature profile

Figure 3a shows the observed vertical profiles of potential temperature and those simulated by the model at Delhi region at 00:00 UTC for six cases out of the nine due to paucity of data. Observed vertical profile of potential temperature is obtained from radiosonde observation taken at Safdarjung Airport, New Delhi, by India Meteorological Department (IMD). Model simulates stable boundary

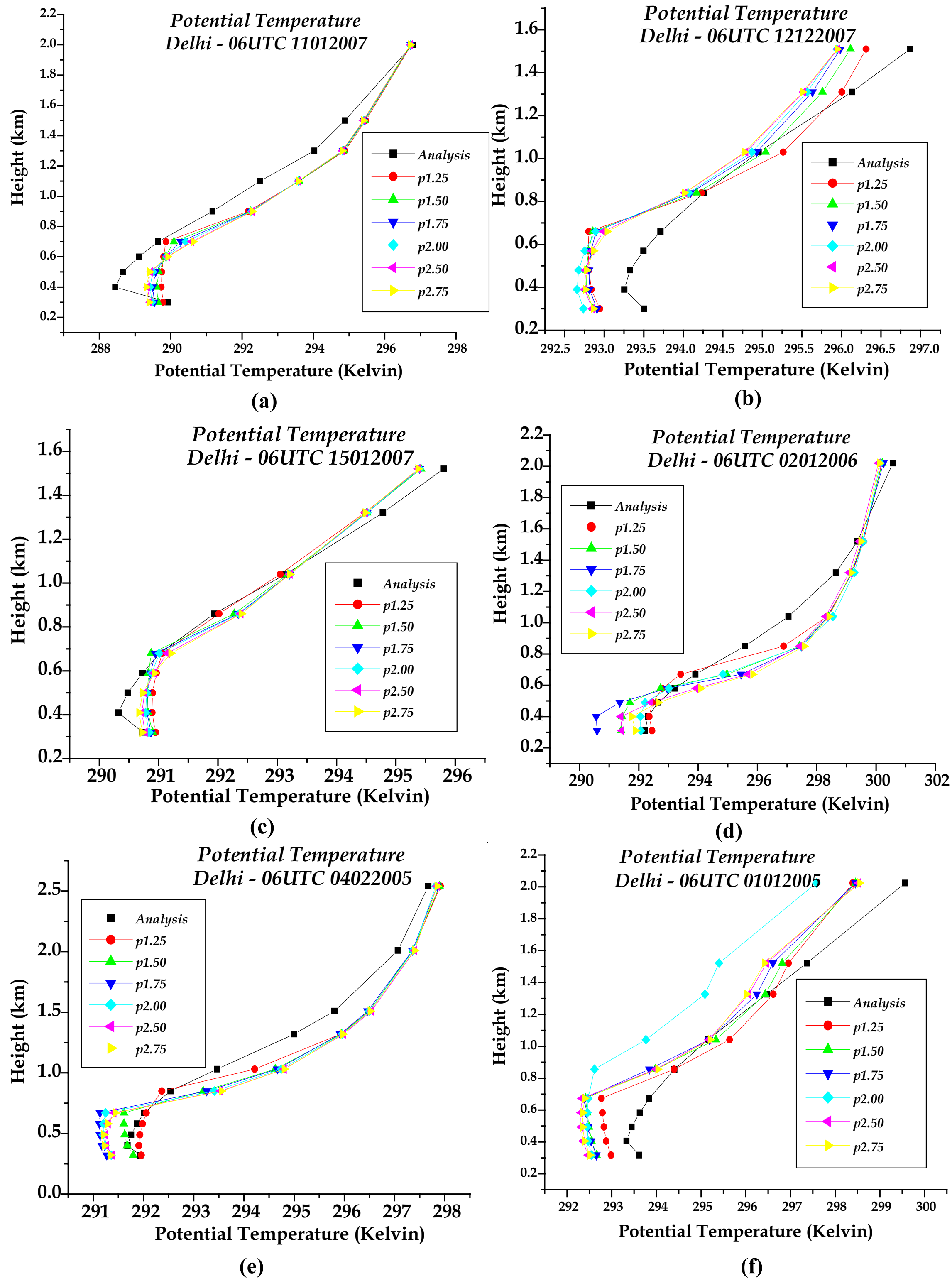

Fig. 4 Potential temperature profile at 06:00 UTC at Delhi for nine cases

layer at 00:00 UTC in all the six cases. Simulated results are in good agreement with the observation except in case 3 (Fig. 3c). In this case, observed profile shows that the atmosphere is in neutral condition in the lowest 1 km. Here, the model is unable to predict the intense mixing at the lower part of the boundary layer due to the local

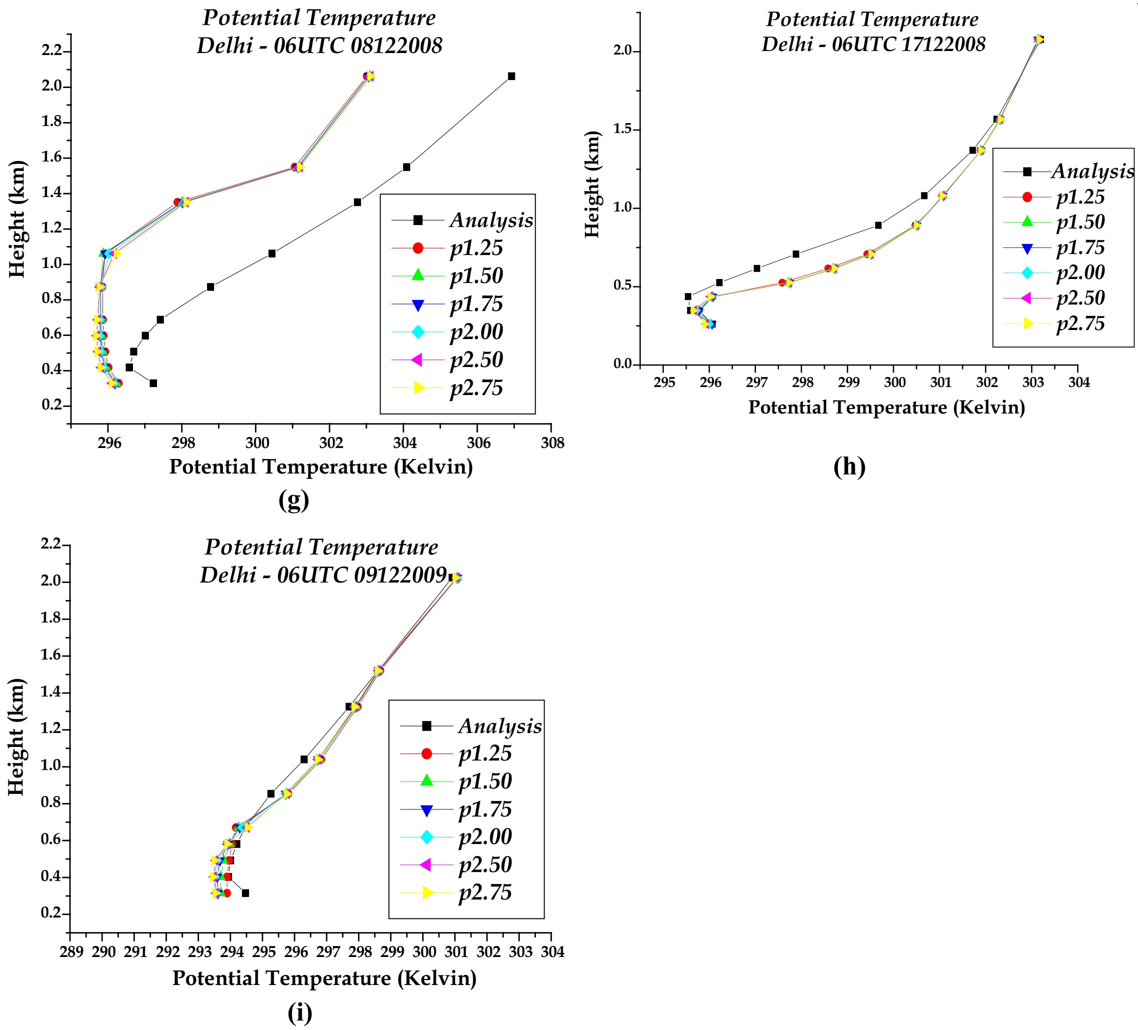

Fig. 4 (continued)

neutral or unstable condition. In cases 2 and 6 (Fig. 3b, d), the model-simulated potential temperature profiles depart appreciably from the observed potential temperature profile. Since in most of the cases atmosphere is stable during early morning hours, the eddy diffusivities are determined by local schemes and hence different values of '*p*' do not have much impact on the potential temperature profiles.

The model-simulated potential temperature profiles for all nine cases of 06:00 UTC at Delhi region have been compared with the analysis profiles in Fig. 4, as the observations are not available at this time of the day. It is to be noticed that at 06:00 UTC, in most of the cases the potential temperatures are different for different values of '*p*' at the lower part of the boundary layer where atmosphere is either neutral or unstable. This is because of the fact that non-local scheme of eddy diffusivity determines the mixing in the boundary layer and different values of '*p*' cause different amounts of mixing. As *p* varies from 1.25 to 2.75, variation of potential temperature becomes as large as 1° K.

In majority of the cases, the potential temperature profile for $p=1.25$ shows closer proximity to the analysis profile within the lowest kilometer of the atmosphere. This reveals that modified formulation of ACM2 with $p=1.25$ is capable of producing adequate mixing of heat flux in the morning neutral condition of lower boundary of the PBL during severe weather phenomenon of WD.

4.2 Impact of '*p*' values on relative humidity profile

Figure 5 shows the model-simulated and IMD-observed relative humidity profiles (obtained from radiosonde observation) over Delhi region at 00:00 UTC for six cases due to non-availability of observational data for other

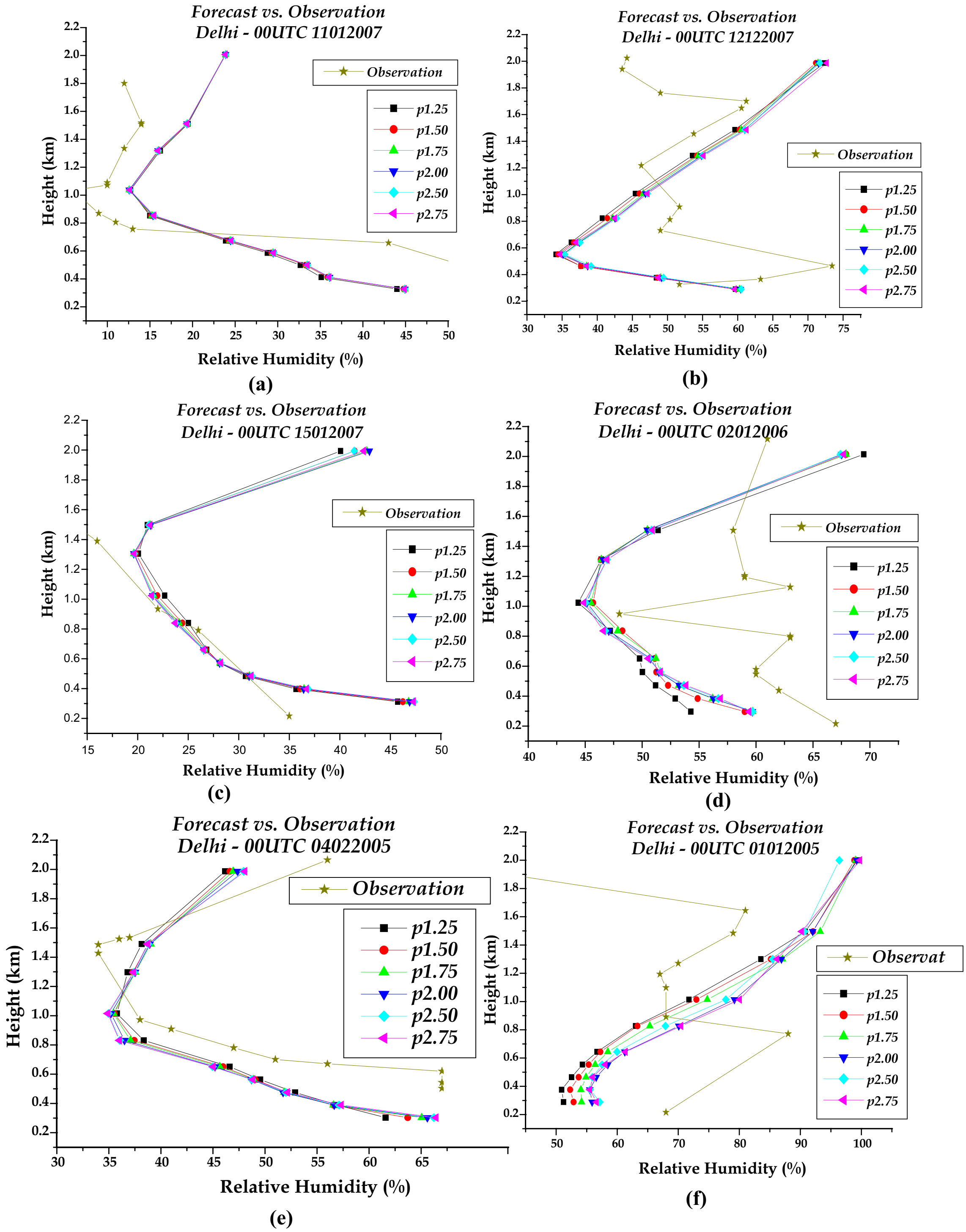

Fig. 5 Relative humidity profile at 00:00 UTC at Delhi for six cases

three cases. Unlike potential temperature, the model-simulated relative humidity shows appreciably larger departure from the observations.

Similarly, the model-simulated and analysis of relative humidity profiles at 06:00 UTC for all nine cases are shown in Fig. 6 over the same place. Here, in most of the cases, the difference between analysis of and model-simulated relative humidity is found significant in the order of ~ 10%. This large difference of simulated relative humidity in the

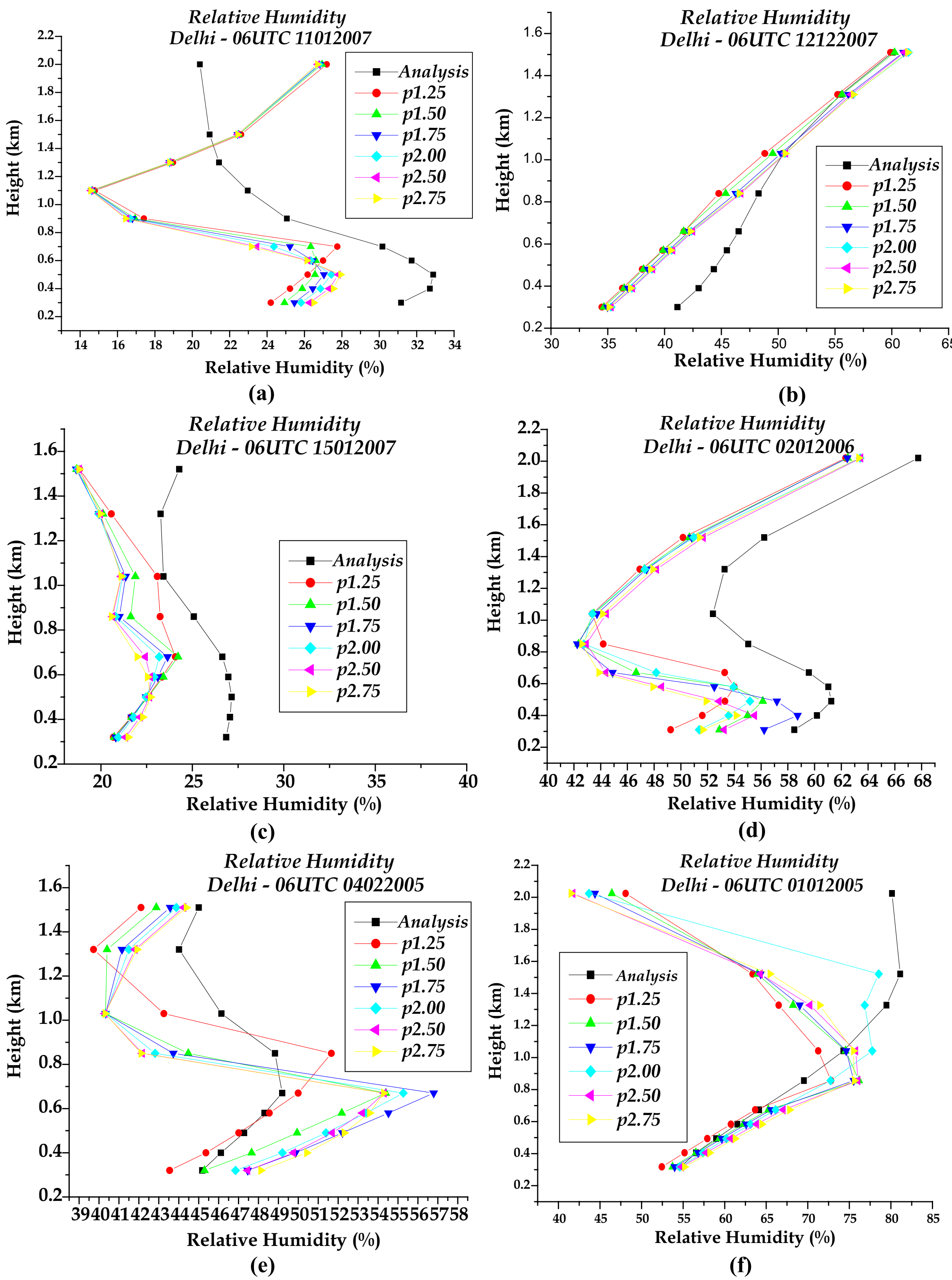

Fig. 6 Relative humidity profile at 06:00 UTC at Delhi for nine cases

order of ~ 10% implies that the modified formulation of ACM2 has minimal ability to produce sufficient mixing of relative humidity (moisture) especially in the morning neutral atmospheric condition during severe weather events. Thus, the model is not efficient in capturing the necessary condition of moisture flux which is a highly variable parameter across the wide spectrum of convection in

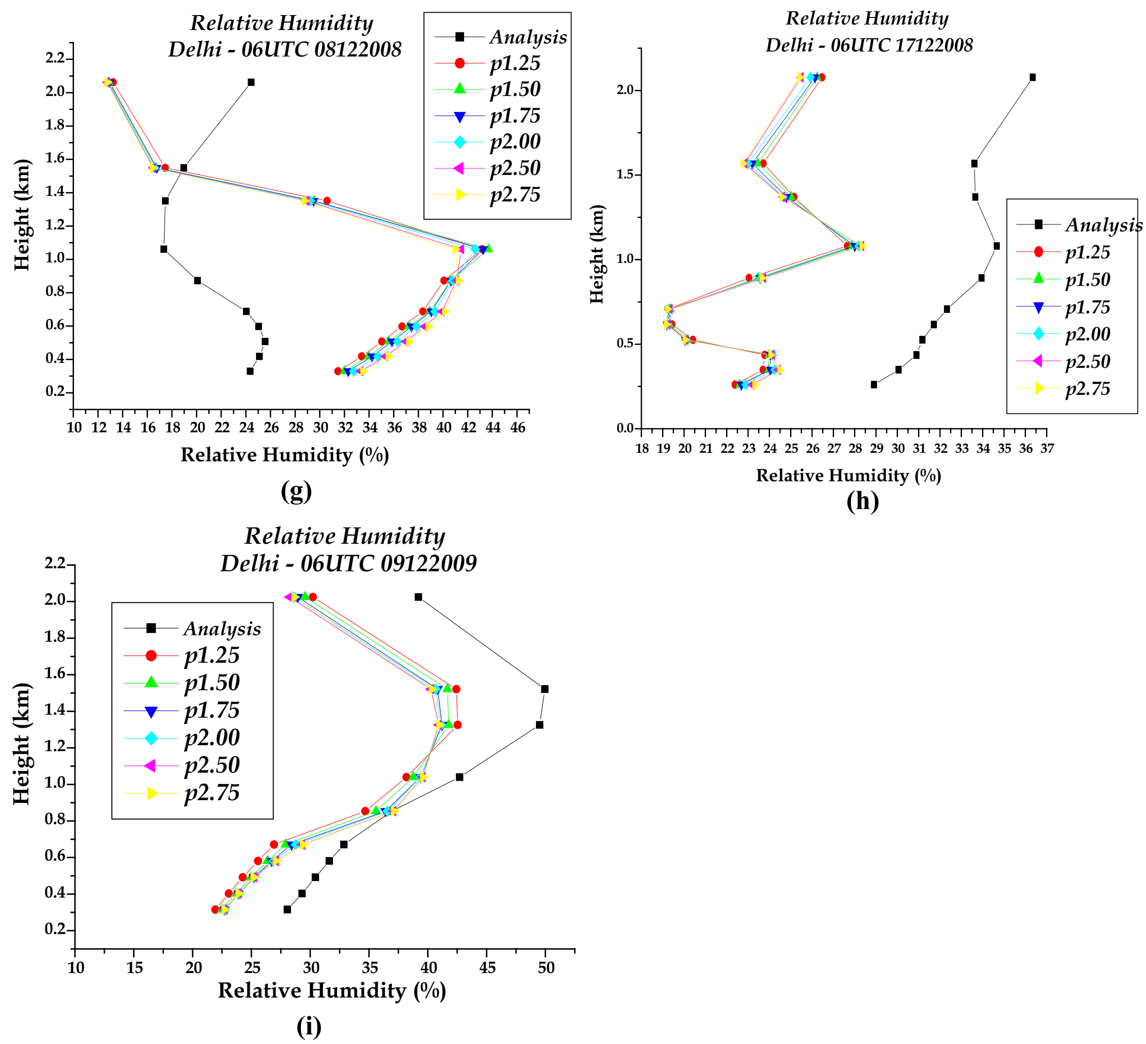

Fig. 6 (continued)

the organized severe weather event. Analysis of the simulated results conveys that other physical processes such as the microphysical processes, cumulus convection process may play more important role to account for the forcing due to turbulence to successfully simulate the relative humidity involved at the lower boundary during neutral or unstable condition of the atmosphere.

4.3 Root-mean-square errors of potential temperature and relative humidity

Figure 7 presents the root-mean-square errors (RMSEs) of potential temperature with respect to analysis up to a height of 1 km. It shows that except in cases 2 and 3, the root-mean-square error of potential temperature corresponding to 'p' = 1.25 is always less than that for other 'p' values. Figure 8 shows that the mean value of RMSE calculated over all the cases is the least and it has a value of 0.86° K while the mean of RMSE corresponding to the default value of p, i.e., 'p' = 2, is 1.04° K.

However, like potential temperature, the root-mean-square error of relative humidity with respect to analysis at 06:00 UTC over Delhi is least for $p = 1.25$ in majority of the cases (see Fig. 9**)**. However, this is highest in cases 2, 8 and 9. The mean value of RMSE calculated over all the cases for relative humidity is also least for $p = 1.25$. Figure 10 shows that the mean value of the domain-averaged RMSE value of relative humidity for $p = 1.25$ is slightly more than 6.68%. The mean RMSE of relative humidity for the default p value (2) is slightly less than 7%. Thus, it can be inferred that the simulated potential temperature and relative humidity profiles for $p = 1.25$ are closest to the respective analysis profiles over Delhi during 06:00 UTC. Thus, the modified formulation of ACM2 scheme by lowering the value of 'p' = 1.25 is sensitive

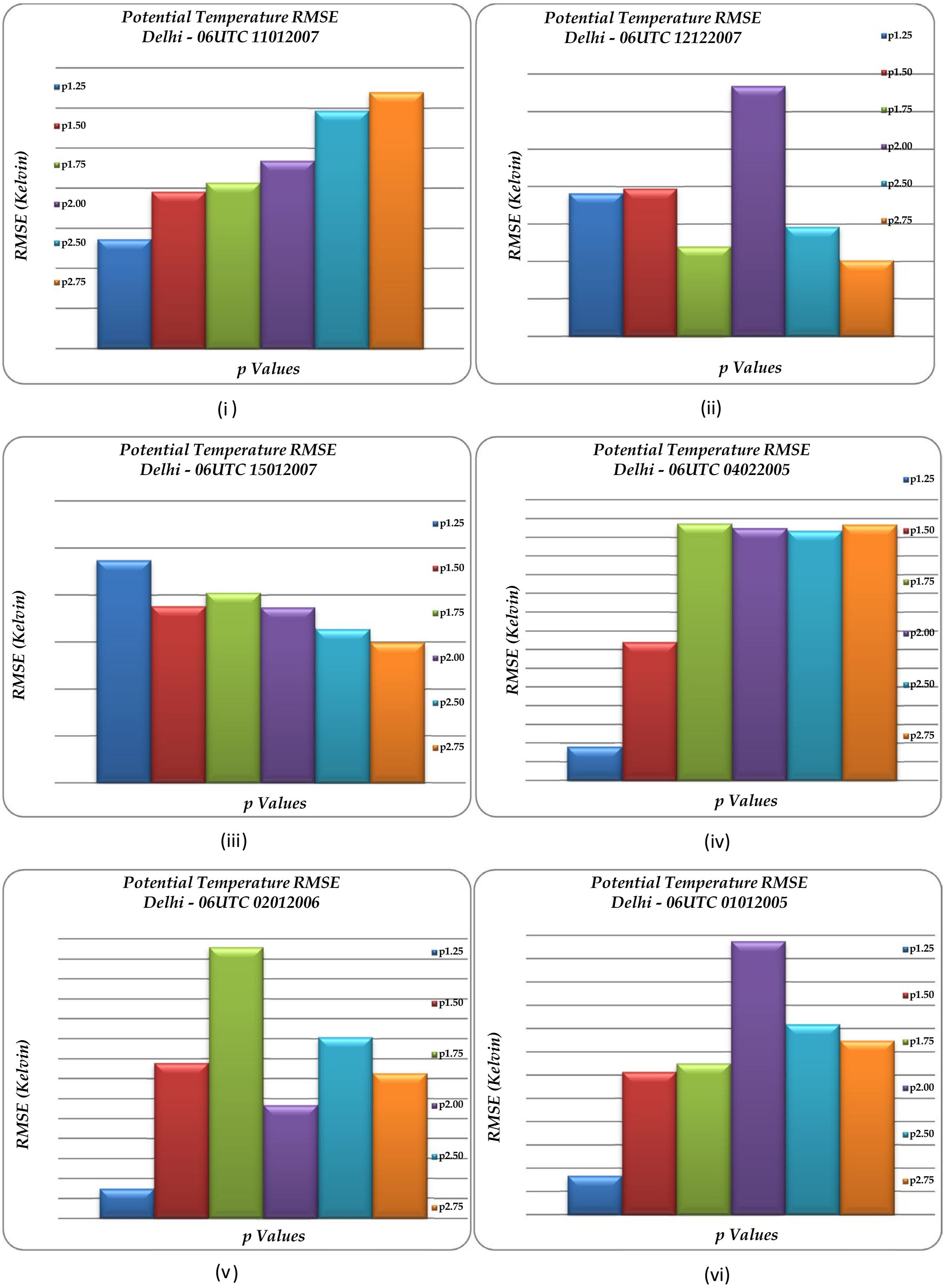

Fig. 7 RMSE of model-simulated potential temperature (*K*) at 06:00 UTC with respect to analysis calculated up to 1 km height at Delhi for all cases

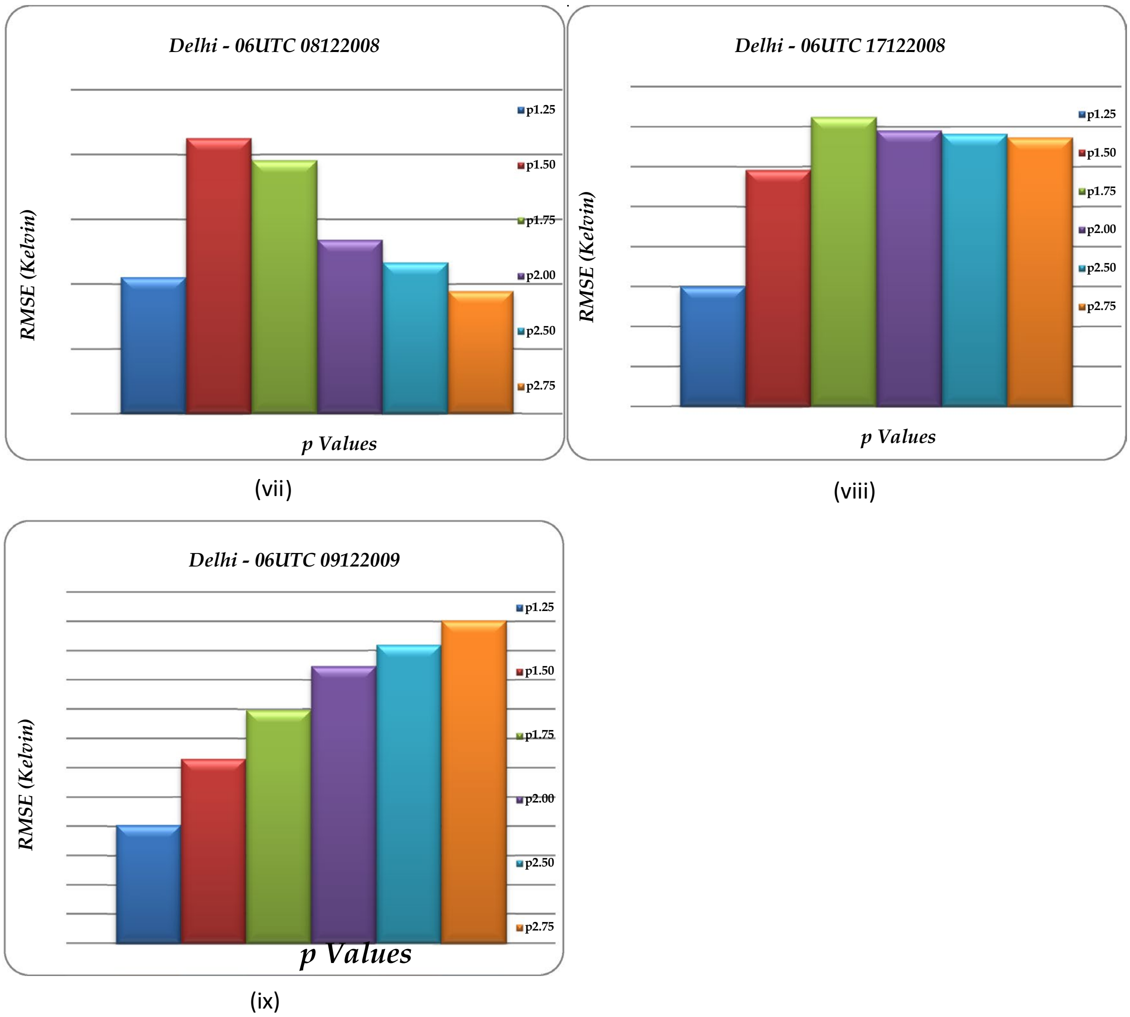

Fig. 7 (continued)

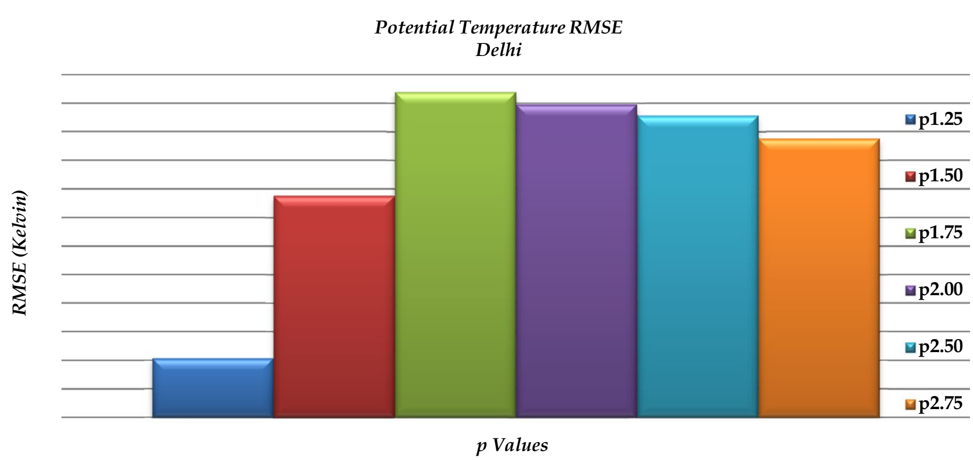

Fig. 8 Mean value of RMSE of potential temperature (*K*) at 06 UTC at Delhi

to the turbulent transport of heat and moisture during convective boundary condition by modifying eddy diffusion. This modified formulation in the ACM2 scheme is perhaps more effective in partitioning of the local and non-local mixing components in the model at least for the domain under study. Therefore, it will be more appropriate to modify the default value of '*p*' to 1.25 in Eq. 1. The

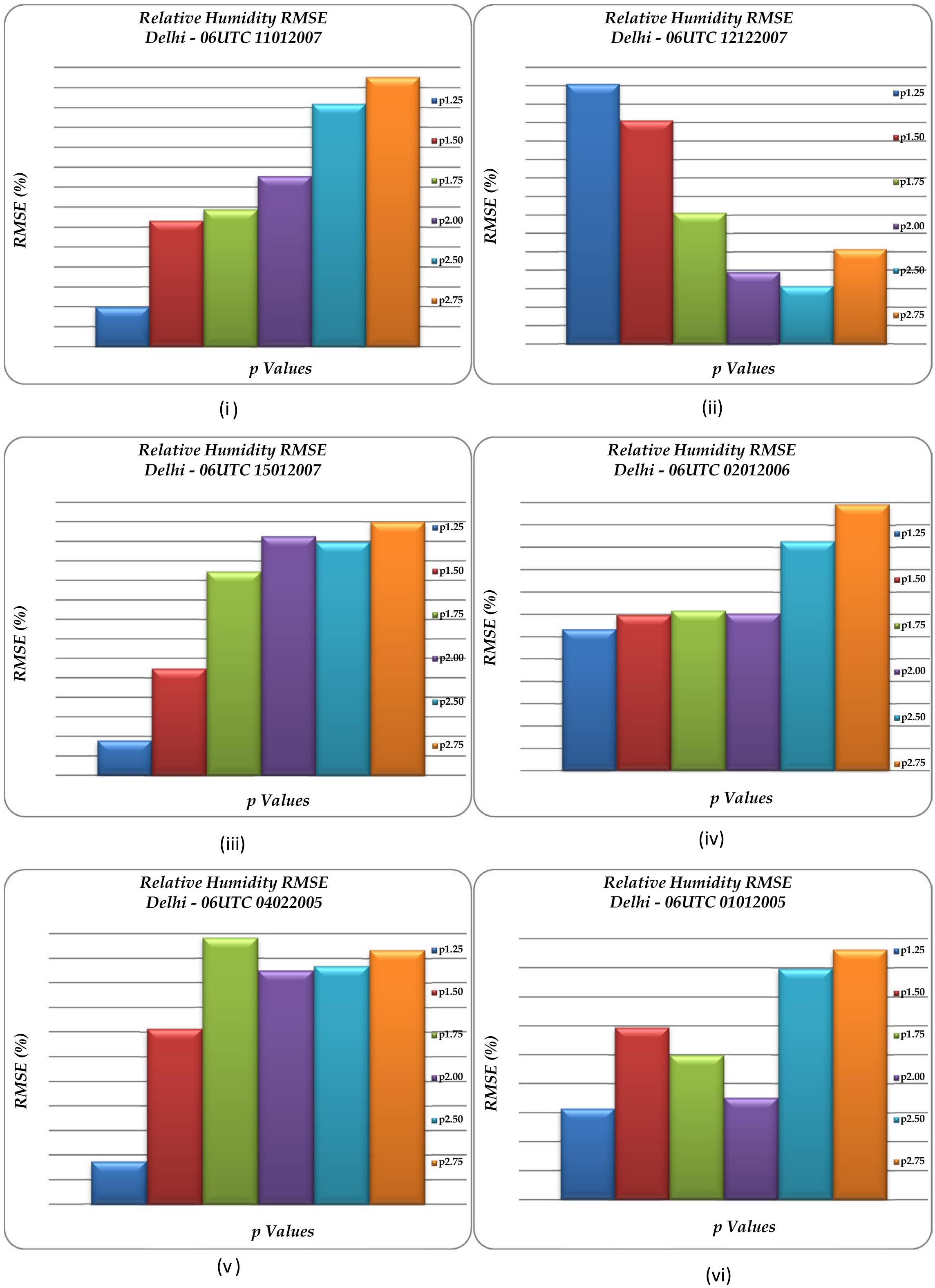

Fig. 9 RMSE of model-simulated relative humidity (%) at 06:00 UTC with respect to analysis calculated up to 1 km height at Delhi for all cases

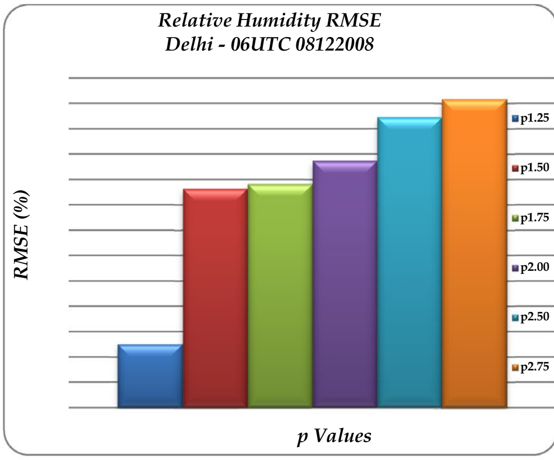

(vii)

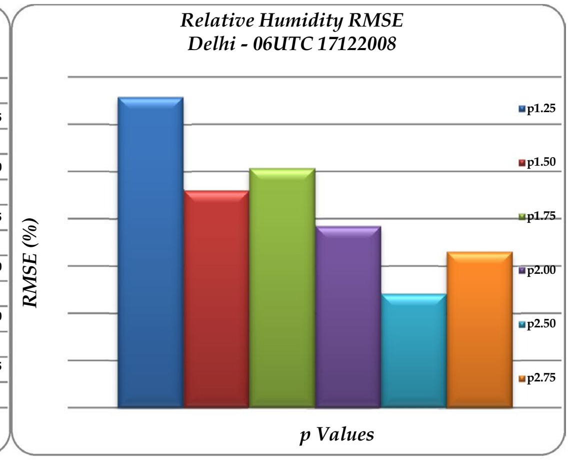

(viii)

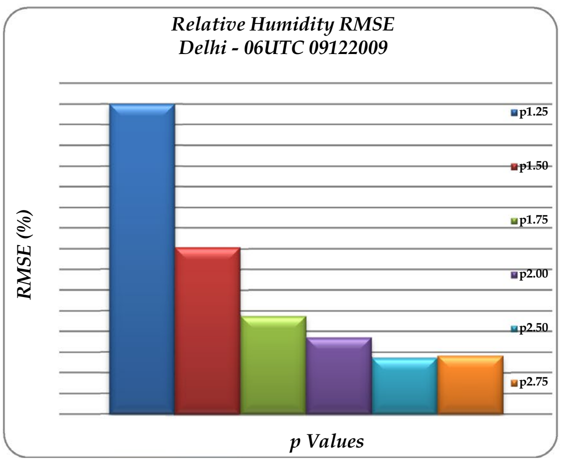

(ix)

Fig. 9 (continued)

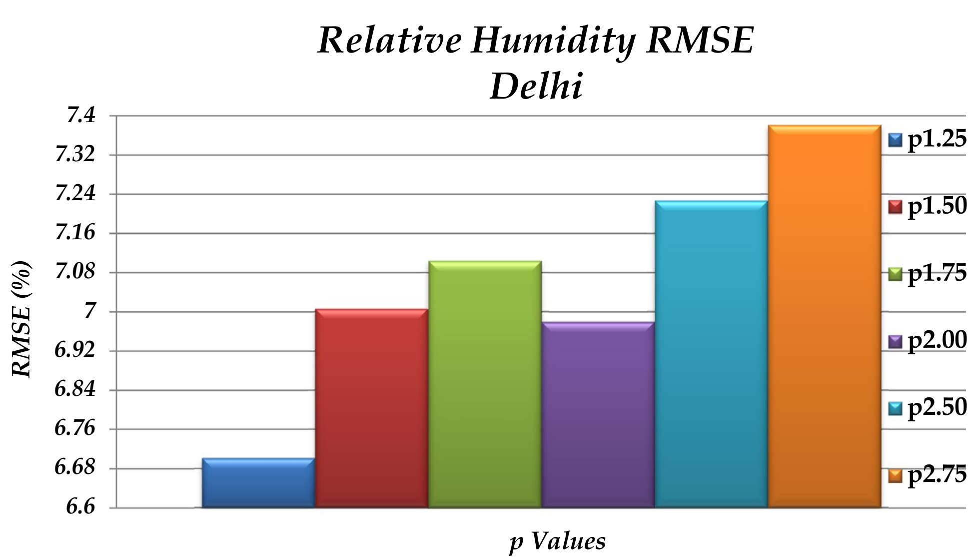

Fig. 10 Mean value of RMSE of relative humidity (%) at 06 UTC at Delhi

default value $p = 2$ may be more applicable for a less convective environment. The lower value of p (=1.25) suitable for the present study indicates that large eddy diffusivity values (and hence larger mixing) are required to represent the convective planetary boundary layer over this tropical region of study. It also indicates that the maximum value of K_z occurs at higher level within boundary layer for $p = 1.25$ than for the default value of p.

5 Conclusion

In the above study, we have presented the results of numerical meteorological simulation for greater area of Northern India at a spatial resolution of 27 km. Sensitivity experiments have been carried out to assess whether WRF-ARW model embedded with ACM2 PBL scheme is capable of correctly reproducing observed meteorological quantities at different values of model hidden parameter '*p*'. To demonstrate this, model-simulated potential temperature and relative humidity profiles over Delhi at 06:00 UTC were compared with analysis data and RMSEs were computed. The comparison shows that $p = 1.25$ scores better than other values of '*p*' for both potential temperature and relative humidity. As a result, we believe that our approach with '*p*' value of 1.25 in the model code is more promising in defining the vertical profile of the PBL especially when one is interested to simulate extreme weather events like WD dominated by convective phenomenon at least for the period and domain under study.

Acknowledgements This project was supported by Department of Science and Technology (DST), Ministry of Science and Technology, Government of India (SR/S4/AS:99/2012). We sincerely thank DST for kindly supporting this project. We are thankful to the principal and the director, Jaipur Engineering College of Research Centre, for providing logistics as well as infrastructural facilities. We are also thankful to the director, National Centre for Medium Range Weather Forecasting, for allowing this project to complete and providing necessary support. We would like to thank India Meteorological Department, New Delhi. We thank National Center for Atmospheric Research (NCAR) for making WRF model and the input data freely available. These have been used to study various western disturbance cases.

Compliance with ethical standards

Conflict of interest The authors declare that they have no conflict of interest.

References

1. Stull RB (1988) An introduction to boundary layer meteorology. Kluwer Academy, Dordrecht
2. Garratt JR (1994) Review: the atmospheric boundary layer. Earth Sci Rev 37:89–134
3. Alapaty K, Alapaty M (2001) Evaluation of a nonlocal-closure K-scheme using the MM5. Workshop program for the eleventh PSU/NCAR MM5 users' workshop. Foothills Laboratory, NCAR
4. Deardorff JW (1972) Theoretical expression for the countergradient vertical heat flux. J Geophys Res 77(30):5900–5904
5. Holtslag AAM, Boville BA (1993) Local versus nonlocal boundary-layer diffusion in a global climate model. J Clim 6:1825–1842
6. Holtslag AAM, Moeng CH (1991) Eddy diffusivity and counter gradient transport in the convective atmospheric boundary layer. J Atmos Sci 48:1690–1698
7. Blackadar AK (1976) Modeling the nocturnal boundary layer. In: 3rd symposium on atmospheric turbulence, diffusion and air quality, Raleigh, NC, 19–22 October 1976. American Meteor Society, pp 46–49 (**Preprints**)
8. Hong SY, Pan HL (1996) Nonlocal boundary layer vertical diffusion in a medium-range forecast model. Mon Weather Rev 124:2322–2339
9. Pleim JE, Chang JS (1992) A non-local closure model for vertical mixing in the convective boundary layer. Atmos Environ 26A:965–981
10. Stull RB (1984) Transilient turbulence theory. Part I: the concept of eddy-mixing across finite distances. J Atmos Sci 41:3351–3367. https://doi.org/10.1175/1520-0469(1984)041%3c3351:TTTPIT%3e2.0.CO;2
11. Pleim JE (2007) A combined local and nonlocal closure model for the atmospheric boundary layer. Part-I: model description and testing. J Appl Meteorol Climatol 46:1381–1395
12. Hu XM, Nielsen-Gammon JW, Zhang F (2010) Evaluation of three planetary boundary layer schemes in the WRF model. J Appl Meteorol Climatol 49:1831–1844. https://doi.org/10.1175/2010jamc2432.1
13. Zhang DL, Zheng WZ (2004) Diurnal cycles of surface winds and temperatures as simulated by five boundary layer parameterizations. J Appl Meteorol 43:157–169
14. Case JL, Crosson WL, Kumar SV, Lapenta WM, Peters-Lidard CD (2008) Impacts of high-resolution land surface initialization on regional sensible weather forecasts from the WRF model. J Hydrometeorol 9:1249–1266
15. Dudhia J (2014) A history of mesoscale model development. Asia Pac J Atmos Sci 50:121–131
16. García-Díez M, Fernández J, Fita L, Yagüe C (2013) Seasonal dependence of WRF model biases and sensitivity to PBL schemes over Europe. Q J R Meteorol Soc 139:501–514
17. Soni M, Payara S, Sinha P, Verma S (2014) A performance evaluation of WRF model using different physical parameterisation scheme during winter season over a semi-arid region, India. Int J Earth Atmos Sci 1(3):104–114
18. Xie B, Fung JCH, Chan A, Lau A (2012) Evaluation of nonlocal and local planetary boundary layer schemes in the WRF model. J Geophys Res 117:D12103. https://doi.org/10.1029/2011jd017080
19. Banks RF, Baldasano JM (2016) Impact of WRF model PBL schemes on air quality simulations over Catalonia, Spain. Sci Total Environ 572:98–113
20. Banks RF, Tiana-Alsina J, Baldasano JM, Rocadenbosch F, Papayannis A, Solomos S, Tzanis CG (2016) Sensitivity of boundary-layer variables to PBL schemes in the WRF model based on surface meteorological observations, lidar, and radiosondes during the HygrA-CD campaign. Atmos Res 10:185–201
21. Boadh R, Satyanarayana ANV, Rama Krishna TVBPS, Madala S (2015) Sensitivity of PBL schemes of the WRF-ARW model in simulating the boundary layer flow parameters for their application to air pollution dispersion modeling over a tropical station. Atmósfera 29(1):61–81. https://doi.org/10.20937/atm.2016.29.01.05

22. Shin HH, Hong SY (2011) Intercomparison of planetary boundary-layer parameterizations in the WRF model for a single day from CASES-99. Bound Layer Meteorol 139(2):261–281
23. Shrivastava R, Dash SK, Oza RB, Sharma DN (2014) Evaluation of parameterization schemes in the WRF model for estimation of mixing height. Int J Atmos Sci, 2014, Article ID 451578. https://doi.org/10.1155/2014/451578
24. Pleim JE (2007) A combined local and nonlocal closure model for the atmospheric boundary layer. Part II: application and evaluation in a mesoscale meteorological model. J Appl Meteorol Climatol 46:1396–1409
25. Nielsen-Gammon JW, Hu XM, Zhang F, Pleim J (2010) Evaluation of planetary boundary layer scheme sensitivities for the purpose of parameter estimation. Mon Weather Rev 138:3400–3417
26. Aksoy A, Zhang F, Nielsen-Gammon JW (2006) Ensemble-based simultaneous state and parameter estimation with MM5. Geophys Res Lett 33:L12801. https://doi.org/10.1029/2006GL026186
27. Hacker JP, Snyder C (2005) Ensemble Kalman filter assimilation of fixed screen-height observations in a parameterized PBL. Mon Weather Rev 133:3260–3275
28. Tong M, Xue M (2008) Simultaneous estimation of microphysical parameters and atmospheric state with simulated radar data and ensemble square root Kalman filter. Part I: sensitivity analysis and parameter identifiability. Mon Weather Rev 136:1630–1648
29. Hong SY, Dudhia J, Chen S-H (2004) A revised approach to ice microphysical processes for the bulk parameterization of clouds and precipitation. Mon Weather Rev 132:103–120
30. Beljaars ACM (1991) Numerical schemes for parameterization. In: Proceedings of the ECMWF seminar on numerical methods in atmospheric models, vol II. ECMWF, Reading, pp 1–42
31. Skamarock WC, Klemp JB, Dudhia J, Gill DO, Barker DM, Duda MG, Huang Z-Y, Wang W, Powes JG (2008) A description of the advanced research WRF version 3. NCAR Technical Notes, NCAR/TN-4751STR. https://doi.org/10.5065/d68s4mvh
32. Sarkar A, Dutta D, Chakraborty P (2017) Numerical diagnosis of situations causing heavy rainfall over the Western Himalayas. Model Earth Syst Environ 3(2):515–531
33. Tanessong RS, Vondou DA, Djomou ZY (2017) WRF high resolution simulation of an extreme rainfall event over Douala (Cameroon): a case study. Model Earth Syst Environ 3(3):927–942
34. Chevuturi A, Dimri AP (2015) Inter-comparison of physical processes associated with winter and non-winter hailstorms using the weather research and forecasting (WRF) model. Model Earth Syst Environ 1:9
35. Patil R, Kumar PP (2016) WRF model sensitivity for simulating intense western disturbances over North West India. Model Earth Syst Environ 2:82
36. Mulukutla ANV, Varghese GK (2015) Comparison of field monitored and prognostic model generated meteorological parameters for source dispersion modeling. Model Earth Syst Environ 1:39
37. Kain JS (2004) The Kain Fritsch convective parameterization: an update. J Appl Meteorol 43(1):170–181
38. Kain JS, Fritsch JM (1990) A one-dimensional entraining/detraining plume model and its application in convective parameterization. J Atmos Sci 47:2784–2802
39. Lin Y-L, Farley RD, Orville HD (1983) Bulk parameterisation of the snow field in a cloud model. J Clim Appl Meteorol 22:1065–1092
40. Chen SH, Sun WY (2002) A one-dimensional time dependent cloud model. J Meteorol Soc Jpn 80:99–118
41. Deardorff JW (1972) Numerical investigation of neutral and unstable planetary boundary layers. J Atmos Sci 29:91–115